Catalysis Today 148 (2009) 70–74

Contents lists available at ScienceDirect

Catalysis Today

journal homepage: www.elsevier.com/locate/cattod

Effect of isopropanol aging of $Zr(OH)_4$ on n-hexane isomerization over Pt-SO_4^{2-}/Al_2O_3–ZrO_2

G.X. Yu [a,b], X.L. Zhou [b,*], F. Liu [b], C.L. Li [b], L.F. Chen [c], J.A. Wang [c]

[a] School of Chemistry and Environmental Engineering, Jianghan University, Wuhan 430056, China
[b] School of Chemical Engineering, East China University of Science & Technology, Meilong Road 130#, Shanghai 200237, China
[c] ESIQIE, Instituto Politécnico Nacional, Av. Politécnico S/N, Col. Zacatenco, 07738 México D.F., Mexico

ARTICLE INFO

Article history:
Available online 15 April 2009

Keywords:
Isopropanol aging
Zirconium hydroxide
Hydroisomerization
n-Hexane
Sulfated zirconia
Alumina

ABSTRACT

Two Pt/SO_4^{2-}/ZrO_2–Al_2O_3 (denoted as PSZA and I-PSZA) catalysts were prepared by using $Zr(OH)_4$ as precursor aged in different conditions, including conventional aging and isopropanol aging. The textural properties, crystalline structure, surface acidity and reduction behaviours of the as PSZA and I-PSZA catalysts were comparatively investigated by N_2 adsorption isotherms, XRD, TG–DSC, pyridine-FTIR and H_2-TPR techniques. Catalytic tests showed that, using isopropanol aged $Zr(OH)_4$ as ZrO_2 precursor, in the n-hexane isomerization reaction, the catalytic activity and stability of the catalyst could be greatly increased and the selectivity of 2,2-DMB was enhanced by more than two times. It was found that isopropanol aging of $Zr(OH)_4$ modified the textural properties and inhibited zirconia phase transformation and stabilized the tetragonal ZrO_2 crystalline structure. On the I-PSZA catalyst, more acid centers were formed in comparison with that presented on the PSZA catalyst. Our experimental results show that the surface acidity, textural properties and phase composition of the Pt/SO_4^{2-}/ZrO_2–Al_2O_3 catalysts play an important role in n-hexane hydroisomerization.

1. Introduction

Hydroisomerization of n-pentane and n-hexane (n-C_5/n-C_6) is one of the most economical and efficient processes to produce high octane number gasoline composition. These reactions are limited by thermodynamic equilibrium, favoring at low temperatures. Platinum loaded mordenite and platinum loaded chlorinated alumina are two kinds of catalysts widely used in the industrial process. The latter catalyst can be operated at lower temperature producing gasoline components with higher octane number, but it needs frequently make-up organic chlorine components, resulting in corrosion and pollution problems. In addition, this catalyst is very sensitive to sulfur and water in the feedstock.

Sulfated zirconia (SZ) promoted with metals demonstrated high catalytic activities in alkane hydroisomerization at low temperatures without the problems and feed limitations mentioned above [1–3]. The strong acidity of SZ has attracted much attention because of its ability to catalyze many reactions, such as cracking, alkylation, and isomerization. For this reason a large number of research works were focused on this catalyst and many reviews are available [4–7]. Nevertheless, SZ showed rapid deactivation during catalytic reactions. Therefore, in recent years, oxides or metals promoted zirconia catalysts have gained much attention for isomerization reactions due to their superacidity, non-toxicity and a high activity at low temperatures [8–11]. A number of transition metals promoters (e.g. Fe, Mn, and Ni) have been added to SZ, resulting in catalysts with higher activity than unmodified SZ [12]. However, rapid deactivation was still observed [12,13] and the marked promoting effect disappeared if the reaction was performed at temperatures higher than 250 °C [14,15]. Recently, it has been found that a main group element Al can also promote the catalytic activity and stability of sulfated zirconia for n-butane and n-hexane isomerization [15–17].

In the catalysis preparation procedure, aging is thought to be related to a process of simultaneous dissolution and precipitation which favors the growth of "neck structures" in the gel network. During this process the support dissolves from regions of positive curvature to redeposit at regions of negative curvature, reinforcing the hydrogel network [18]. This lattice refining removes brittle structures and a more homogeneous network is produced. SEM images of materials aged in aqueous medium or in molten salt baths reveal a "cheese" like structure [19].

In this paper, the effects of isopropanol aging of $Zr(OH)_4$ on the textural structures, ZrO_2 crystallization process, surface acidity, reduction of the sulfur species and catalytic performance of PSZA catalysts were studied.

* Corresponding author. Tel.: +86 21 64252041; fax: +86 21 64253049.
E-mail address: xiaolong@ecust.edu.cn (X.L. Zhou).

0920-5861/$ – see front matter © 2009 Elsevier B.V. All rights reserved.
doi:10.1016/j.cattod.2009.02.045

2. Experimental

2.1. Catalyst preparation

A solution with zirconium concentration of 0.4 mol l^{-1} was prepared by dissolving $ZrOCl_2{\cdot}8H_2O$ in deionized water. A 26 wt.% ammonia solution was dropwise added into that solution at a rate of 0.5 ml/min up to pH of 10. The mixture was separated into two portions. One portion was filtered after being aged for 24 h at 25 °C, and the other was mixed with isopropanol of equal volume for aging at 25 °C for 24 h, and then it was filtered. These two precipitates were washed with distilled water until the disappearance of chloride ions ($AgNO_3$ test); and dried at 110 °C for 12 h. The obtained $Zr(OH)_4$ samples (the sample of isopropanol treatment was designated as I-$Zr(OH)_4$) was shaped with boehmite (alumina content is 5.0 wt.% in the mixed oxides). The shaped solid samples were dried at 110 °C and then pulverized to particles smaller than 290 μm.

Sulfation procedure was carried out by impregnation method with 0.5 mol l^{-1} of H_2SO_4 solution (15 ml g^{-1}) under continuous stirring at room temperature for 12 h. The sulfated boehmite–$Zr(OH)_4$ solids were filtered without washing then dried overnight at 110 °C, and then the dry sulfated solid samples were calcined at 625 °C (designated as SZA and I-SZA). Subsequently, the above products were impregnated with H_2PtCl_6 solution using the incipient wetness technique, and the time remaining at ambient temperature is 24 h. It was then dried overnight at 110 °C before the final calcination at a fixed temperature of 525 °C for 2 h. The platinum content was 0.5 wt.%. The obtained Pt-SO_4^{2-}/ZrO_2–Al_2O_3 catalysts were designated as PSZA and I-PSZA.

2.2. Catalyst characterization

The surface areas and pore diameters of the catalysts were measured by N_2 adsorption–desorption isotherms method at −196 °C with a Micromeritics ASAP 2010 instrument. Prior to analysis, each sample was degassed at 200 °C for 6 h under 10^{-3} Torr. Specific surface areas were calculated by BET method and the pore size distribution patterns were obtained from the analysis of the desorption portion of the isotherms using the BJH method.

The powder X-ray diffraction (XRD) patterns were recorded on a Rigaku D/Max 2550 X using Cu Kα(l = 0.154 nm) radiation in an operating mode of 40 kV and 30 mA. Data were collected from 2-theta = 5–75° in steps of 0.02°/s.

Thermogravimetric (TG) and differential scanning calorimetric (DSC) analyses were performed on a SDT-Q600 instrument (TA, USA) in flowing air with temperature ramp set at 10 °C/min in the range from 25 °C to 1000 °C temperature.

Fourier-transform infrared (FTIR) spectra of adsorbed pyridine were recorded on a Bruker IES-88 spectrometer. The sample was pressed to a 15 mm plate and put in a wafer. It was degassed in vacuum of 10^{-4} Torr at 450 °C for 2 h and lowered the IR cell temperature to 200 °C. Pyridine was adsorbed for 10 min and took 30 min for equilibrium. Then it was scanned after being vacuumed for 40 min. Then raised the temperature to 300 °C and recorded after 10 min for equilibrium. The same procedures were carried out at 400 °C and 450 °C. The number of Brönsted and Lewis acid sites was calculated according to the integral area of the bands at 1540 cm^{-1} and 1450 cm^{-1}, respectively.

H_2-temperature programmed reduction (TPR) experiments were performed in Auto Chem II (Micromeritics, USA). The heating rate was 10 °C/min from 50 °C to 900 °C using argon stream containing 7 vol.% hydrogen. The hydrogen consumption was measured by a Shimadzu GC-8A gas chromatograph, equipped with a thermal conductivity detector (TCD).

2.3. Catalytic reaction

The n-hexane hydroisomerization reaction was carried out in a flow-type fixed-bed reactor loaded with 1.0 g of catalyst. Prior to the reaction, the catalyst sample was pretreated with flowing dry air (40 ml/min) at 450 °C for 3 h to remove water adsorbed on the surface. The system was cooled to 250 °C and the catalyst was reduced in flowing hydrogen for 3 h at 250 °C. Hydrogen and n-hexane mixture was then introduced into the reactor and hydroisomerization evaluations were carried out under a total pressure of 2.0 MPa at the desired temperature with n-hexane weight hourly space velocity (WHSV) of 2.0 h^{-1} and a hydrogen/n-hexane molar ratio of 3.0. Products were monitored and analyzed using an on-line GC-920 gas chromatograph.

3. Results and discussion

3.1. Catalytic tests

The n-hexane hydroisomerization reactions were performed over PSZA and I-PSZA catalysts at the temperature ranging from 190 °C to 260 °C. The conversion and iso-hexane yields were given in Fig. 1. It is seen from Fig. 1(a) that the n-hexane conversion over I-PSZA is higher than that over PSZA at the temperature ranging from 190 °C to 260 °C. The iso-hexanes yield over I-PSZA reaches the maximum at 220 °C, approximately 80%, as shown in Fig. 1(b). It was shown that isopropanol aging of $Zr(OH)_4$ increased both n-hexane conversion and isomerization selectivity over PSZA catalyst.

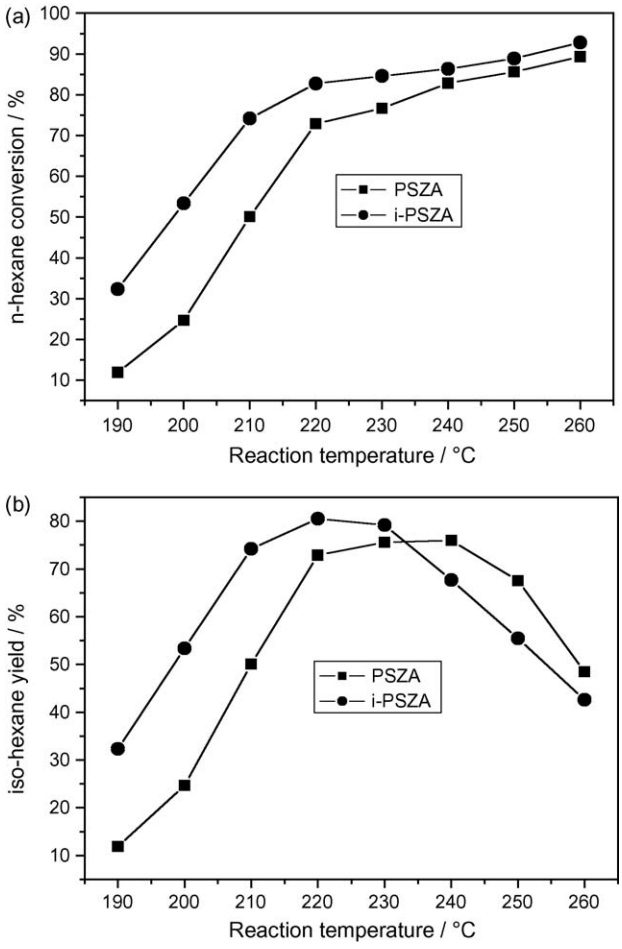

Fig. 1. Effect of reaction temperature on n-C6 hydroisomerization over catalysts.

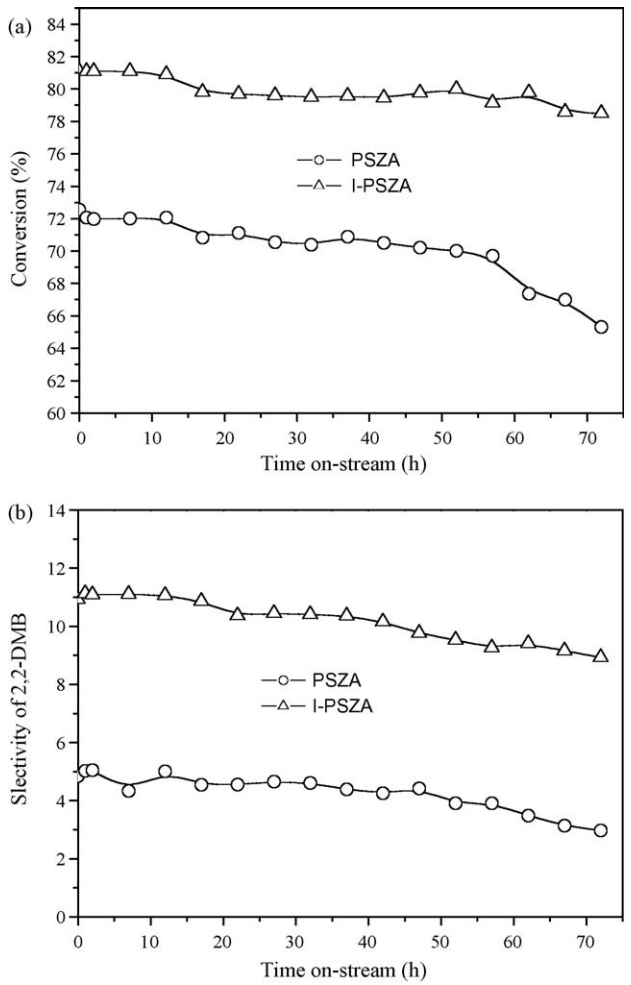

Fig. 2. n-C6 hydroisomerization over catalysts.

The catalytic stability of the catalysts was also evaluated at 220 °C for 72 h. The n-hexane conversion and 2,2-DMB selectivity of the catalysts were shown in Fig. 2. It was seen that the n-hexane conversion over I-PSZA slightly dropped during 72 h of time on stream, however, after 55 h of reaction, the conversion over PSZA obviously decreased, as shown in Fig. 2(a). In addition, over I-PSZA catalyst, selectivity of 2,2-DMB, a high octane rating isomerization product, increased to more than two times at the initial reaction stage after isopropanol aging of $Zr(OH)_4$, as shown in Fig. 2(b). 2,2-DMB selectivity over two PSZA catalysts decreased as reaction time increased, however, 2,2-DMB selectivity over I-PSZA was still higher, and reached 8.93% after 72 h of time on stream, and the corresponding selectivity over PSZA is 2.97%. According to our experimental results in Fig. 2, after 55 h of time on stream, the activity reduced much faster than 2,2-DMB selectivity did for PSZA catalyst. It was because, for n-hexane isomerization, the factors impacting catalytic activity are not all identical to those affecting 2,2-DMB selectivity. Therefore, it is concluded that isopropanol aging of $Zr(OH)_4$ has an important impact on the catalytic performance of I-PSZA, enhancing the catalytic activity and isomerization selectivity.

3.2. Textural property and crystalline structures and catalytic activity

Textural data of two $Zr(OH)_4$ samples and two catalysts (PSZA and I-PSZA) were listed in Table 1. It was seen that BET surface area of isopropanol aged $Zr(OH)_4$ was as double as that of the untreated sample, and also isopropanol treatment led to an increase in the pore diameter of $Zr(OH)_4$. In addition, BET surface and pore diameter of the I-PSZA catalyst are bigger than that of the PSZA. These suggested that isopropanol aging obviously modified the textural structures of the solid, probably because isopropanol prevented agglomeration of colloidal $Zr(OH)_4$ particles during the aging process. Organic solvents are preferred for the preparation of nanoparticles. They perform stabilizing functions. Such solvents or surfactants play a key role in the synthesis of nanoparticles. They are bound to the surface of growing nanocrystals via polar groups, form complexes with species in solutions and control their chemical reactivity and diffusion to the surface of a growing particle [20]. Isopropanol is an organic solvent, it plays the above-mentioned roles. During the aging, isopropanol may replace adsorbed water around the zirconium hydroxide colloidal particle surfaces, thereby inhibiting the agglomeration of the colloidal particles.

Table 1
Textural structures of samples.

Samples	S_{BET} ($m^2\ g^{-1}$)	Pore diameter (nm)
$Zr(OH)_4$	280	3.03
I-$Zr(OH)_4$	560	4.85
PSZA	105	4.42
I-PSZA	135	7.00

XRD patterns of the samples calcined at 625 °C and 700 °C were shown in Fig. 3. For the catalyst PSZA calcined at 625 °C, only tetragonal zirconia phase was formed, however, when it was calcined at 700 °C, a small peak at 2-theta of 28.18° appeared, indicating that trace amount of monoclinic phase was also formed. For the catalyst I-PSZA calcined at 625 °C and 700 °C, only well-defined peaks corresponding to tetragonal zirconia phase were observed. In addition, the peak intensity of the catalyst I-PSZA remained unchanged when the calcination temperature increased from 625 °C to 700 °C, indicating that the crystallite size remained the same, which differed from the PSZA solid where the corresponding peaks became sharper. In the PSZA catalyst, a small peak corresponding to monoclinic zirconia phase appeared at around at 2-theta of 28.18°, indicating that phase transformation from tetragonal to monoclinic took place. Therefore, isopropanol aging of $Zr(OH)_4$ may effectively inhibit ZrO_2 phase transformation and resist crystal growth and thus stabilize the tetragonal zirconia structure. It has been commonly recognized that the crystalline phase of the SZ catalysts plays a very important role in catalytic activity and the zirconia with tetragonal structure shows a higher catalytic activity than that of monoclinic ZrO_2 structure in alkane

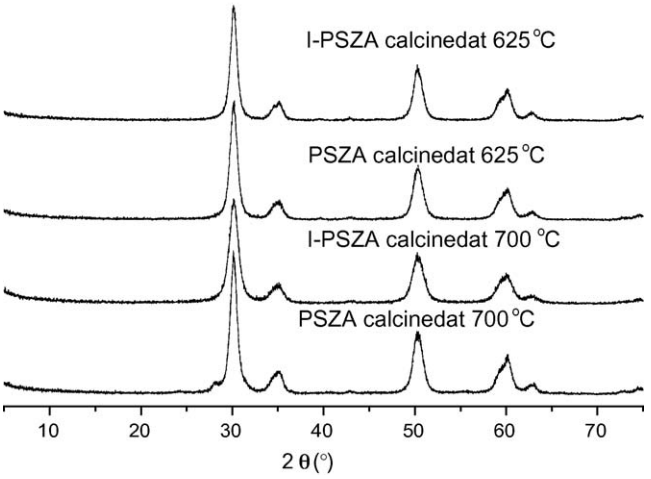

Fig. 3. XRD patterns of the catalysts.

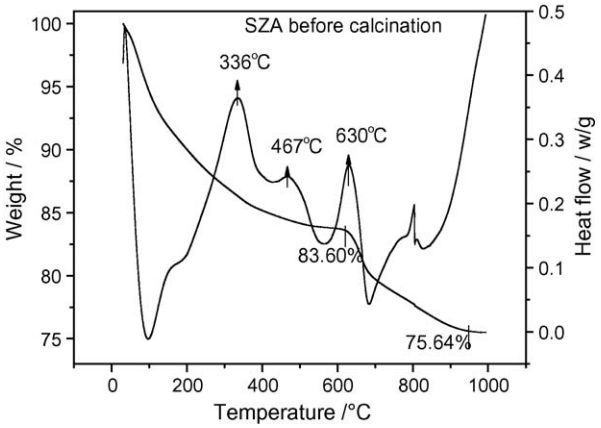

Fig. 4. TG–DSC curve of uncalcined SZA sample.

isomerization [21,22]. The enhancement of the catalytic activity and isomerization selectivity of the I-PZSA catalyst has a close relation to the phase composition and crystalline structure.

3.3. TG–DSC analyses of SZA and I-SZA

Thermal analysis results for SZA and I-SZA before calcination were presented in Figs. 4 and 5. The TG curve of SZA exhibited several weight loss stages. The first weight loss stage accompanying a strongly endothermic process between 100 °C and 200 °C, was resulted from the removal of physic-adsorbed water and ammonia; the second weight loss stage, ranging from 200 °C to 533 °C, was assigned to dehydroxylation step and boehmite decomposition according to the following reaction:

$$2AlOOH \rightarrow Al_2O_3 + H_2O \quad (1)$$

In the third stage, weight loss between 550 °C and 620 °C was produced, it corresponded to $Zr(OH)_4$ decomposition or zirconia crystallization procedure:

$$Zr(OH)_4 \rightarrow ZrO_2 + H_2O \quad (2)$$

In the last weight loss stage at a temperature range between 620 °C and 943 °C was due to decomposition of sulfates [23,24]. The corresponding weight loss in the last stage was around 7.96 wt.%.

Similarly, the TG curve of I-SZA before calcination consisted of four weight loss regions, they were respectively assigned to desorption of physic-adsorbed water, isopropanol and ammonia in the temperature range between 25 °C and 200 °C, to dehydroxylation and boehmite decomposition in the second stage between 200 °C and 519 °C, to the crystallization of zirconium oxide in the third stage and to sulfates decomposition in the last stage between 620 °C and 934 °C. The weight percentage of SO_4^{2-} in I-SZA accounted for 8.79 wt.%. The TG analysis results showed that the sulfate content in I-SZA is higher than that in SZA.

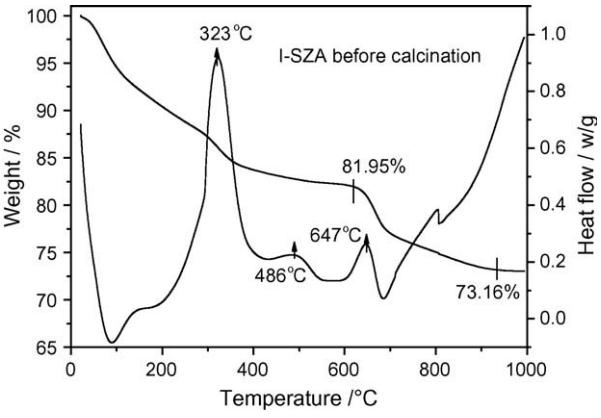

Fig. 5. TG–DSC curve of uncalcined I-SZA sample.

DSC curves, reported in Figs. 4 and 5, provide complementary information. For DSC curves of Fig. 4, the low exothermic peak at 336 °C should be assigned to the boehmite decomposition while the dehydroxylation procedure went on; meanwhile, other two exothermic peaks at 467 °C and 630 °C should be assigned to ZrO_2 crystallization which was accomplished around 630 °C; moreover, the exothermic peak at 630 °C demonstrated predominant crystallization of amorphous zirconium hydroxide resulting in crystalline ZrO_2 network. For DSC curves of Fig. 5, the exothermic peak at 323 °C should be assigned to AlOOH decomposition and dehydroxylation of zirconium hydroxide; meanwhile, other two exothermic peaks at 486 °C and 647 °C should also be assigned to ZrO_2 crystallization which was accomplished around 647 °C. It was reported that the crystallization of ZrO_2 was delayed by sulfated on amorphous zirconium hydroxide [25]. The addition of alumina to zirconia can retard the transformation of metastable tetragonal zirconia phase into more stable monoclinic phase [26].

3.4. Surface acidity and catalytic activity

Surface acidities including the number of the acid sites and acidity strength are the most important features of the acidic catalysts in n-alkane isomerization reaction. Many reports had focused on the identification of different acid sites of sulfated zirconia [4,27–29] and showed the coexistence of Brönsted and Lewis acid sites on the surface [30]. The number and strength of these acid sites vary with factors such as sulfur concentration, activation temperature, and surface area of the samples and could be determined by using IR spectrum of adsorbed pyridine technique [31,32].

Acidities of PSZA and I-PSZA measured by FTIR characterization using pyridine as a probe base were shown in Table 2, where three kinds of acid sites with varying strengths were separated. The acid sites measured at 200 °C were assigned to weak acid sites, those at 300 °C were moderately strong acid sites, whereas that at 400 °C and 450 °C were assigned to superacid sites. It showed that numbers of Brönsted acid sites in the catalyst I-PSZA are higher than those in the catalyst PSZA, and numbers of Lewis acid sites in the catalyst I-PSZA are higher, too; moreover, analyzing acid sites change for the PSZA catalysts, it was seen that the increase in numbers of Lewis acid sites is higher than that in Brönsted acid sites after isopropanol aging of $Zr(OH)_4$. For example, numbers of

Table 2
Acidity data of the catalysts from FTIR spectra of adsorbed pyridine and the acidity density (D_A).

Desorption Temperature	Desorption amount	I-PSZA	PSZA	D_A (μmol/m^2)	
				I-PSZA	PSZA
200 °C (μmol g^{-1})	B acid	55	38	0.410	0.362
	L acid	255	171	1.903	1.276
	Total acid	310	209	2.313	1.560
300 °C (μmol g^{-1})	B acid	44	28	0.328	0.267
	L acid	175	121	1.306	1.152
	Total acid	219	149	1.634	1.419
400 °C (μmol g^{-1})	B acid	30	19	0.224	0.181
	L acid	108	81	0.806	0.771
	Total acid	138	100	1.030	0.952
450 °C (μmol g^{-1})	B acid	23	14	0.172	0.133
	L acid	83	63	0.619	0.600
	Total acid	106	77	0.791	0.733

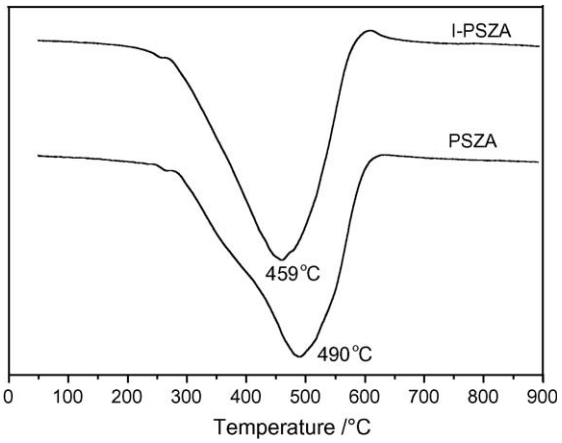

Fig. 6. H_2-TPR profiles of the sample.

Lewis acid sites in the catalyst I-PSZA were 108 μmol g^{-1} and 83 μmol g^{-1}, at 400 °C and 450 °C respectively, corresponding numbers of them for PSZA were 81 μmol g^{-1} and 65 μmol g^{-1}. Therefore, relative to PSZA, more Lewis acid sites were achieved on the I-PASZ catalyst. Similarly, an increment in numbers of Brönsted acid sites are also observed on I-PASZ, by 11 μmol g^{-1} at 400 °C and 9 μmol g^{-1} at 450 °C, respectively. From D_A data in Table 2, all acid densities in the catalyst I-PSZA are higher than those in the catalyst PSZA. So isopropanol aging of $Zr(OH)_4$ obviously increased the acid site density of the catalyst. As reported above, the catalytic activity and isomerization selectivity of the I-PSZA catalyst are superior to the PSZA catalyst, which also can be correlated with its enhanced surface acidity.

3.5. Sulfate reducibility and catalytic activity

TPR profiles of the two PSZA catalysts are shown in Fig. 6. It is seen that only one peak with quite similar area appeared at each of these two traces. It was ascribed to the reduction of sulfate ions from the literatures [6,33–35]. No peak was detected at temperature around 200 °C that resulted from Pt oxide reduction to metallic state [6]. Ebitani et al. [33,34] suggested the absence of a distinct low-temperature reduction peak for platinum oxide can be because platinum is present as sulfide or sulfate that is harder to reduce. The Pt reduction is then delayed in the TPR, and is masked by the dominant sulfur reduction [35]. The results shown in Fig. 6 indicated that isopropanol aging of $Zr(OH)_4$ led to a higher reducibility of the sulfur species on I-PSZA.

It was reported that transition metal, like Fe [36] and Ga [2] and Pt [35,37] promoted SZ would possess higher sulfate reduction ability in H_2-TPR compared to SZ and the sulfate reduction ability was in line with catalytic activity. The differences in the sulfate reduction ability between the PSZA and I-PSZA catalysts, however, might not result from platinum behaviour itself, because two SZA and I-SZA samples were calcined at same temperature, and the final calcination of the PSZA catalysts after Pt loading was performed at a fixed temperature viz. 525 °C. It is assumed that the lower the peak temperature of reduction of surface sulfates of the catalysts is, the more active the sulfates would be, and which would lead to higher catalytic activity in the isomerization reaction as shown in Fig. 1. Therefore it was postulated that the catalytic performance differences partially originated from the different surface property of the SZA and I-SZA catalysts, especially their surface acid properties. In H_2-TPR tests, there were possibilities that the stronger surface acids resulted in easier sulfate reduction by electron addition from Pt particles.

4. Conclusions

Isopropanol aging of $Zr(OH)_4$ could modify the textural properties of I-PSZA catalyst and resisted zirconia crystal growth as well as inhibited zirconia phase transformation, probably because isopropanol would prevent colloidal $Zr(OH)_4$ particles from agglomeration during the aging process. Compared with PSZA catalyst, the I-PSZA catalyst not only contained more sulfur species on the surface and thus exhibited higher acid site density, but also promoted the sulfate reduction ability. In n-hexane hydroisomerization, the enhancement of the catalytic activity and stability and the isomerization selectivity of the catalyst by using isopropanol aged $Zr(OH)_4$ can be largely correlated with its increased surface acidic density, and modified textural properties and improved crystalline structures.

Acknowledgement

We would like to thank the financial supports from the key international cooperative research projects by National Ministry of Science and Technology, PR China (No. 2004CB720603).

References

[1] A. Jatia, C. Chang, J.D. Macleod, T. Okubo, M.E. Davis, Catal. Lett. 25 (1994) 21.
[2] J.C. Yori, J.M. Parera, Appl. Catal. A: Gen. 147 (1996) 145.
[3] C.J. Cao, S. Han, C.L. Chen, N.P. Xu, C.Y. Mou, Catal. Commun. 4 (2003) 511.
[4] T. Yamaguchi, Appl. Catal. 61 (1990) 1.
[5] A. Corma, Chem. Rev. 95 (1995) 559.
[6] X.M. Song, A. Sayari, Catal. Rev. Sci. Eng. 38 (1996) 320.
[7] T.K. Cheung, B.C. Gates, Top. Catal. 6 (1998) 41.
[8] K. Föttinger, E. Halwax, H. Vinek, Appl. Catal. A: Gen. 301 (2006) 115.
[9] R. Akkari, A. Ghorbel, N. Essayem, F. Figueras, Appl. Catal. A: Gen. 328 (2007) 43.
[10] M. Busto, K. Shimizu, C.R. Vera, J.M. Grau, C.L. Pieck, M.A. D'Amato, M.T. Causa, M. Tovar, Appl. Catal. A: Gen. 348 (2008) 173.
[11] J.H. Wang, C.Y. Mou, Micropor. Mesopor. Mater. 110 (2008) 260.
[12] M.A. Coelho, D.E. Resasco, E.C. Skabwe, R.L. White, Catal. Lett. 32 (1995) 256.
[13] V. Adeeva, J.W. de Haan, J. Jänchen, G.D. Lei, V. Schunemann, L.J.M. van de Ven, W.M.H. Sachtler, R.A. van Santen, J. Catal. 151 (1995) 364.
[14] Z. Gao, Y.D. Xia, W.M. Hua, C.X. Miao, Top. Catal. 6 (1998) 101.
[15] W.M. Hua, Y.D. Xia, Y.H. Yue, Z. Gao, J. Catal. 196 (2000) 104.
[16] J.A. Moreno, G. Poncelet, J. Catal. 203 (2001) 153.
[17] G.X. Yu, X.L. Zhou, C. Tang, C.L. Li, J.A. Wang, O. Novaro, Catal. Commun. 9 (2008) 1770.
[18] H.E. Bergna, Ullmann's Encyclopedia of Industrial Chemistry, fifth ed., VCH, Weinheim, 1993.
[19] P. Afanasiev, C. Geantet, M. Lacroix, M. Breysse, J. Catal. 162 (1996) 143.
[20] G.B. Sergeev, Nanochemistry, Elsevier, Amsterdam, 2006.
[21] S.Y. Kim, J.G. Goodwin, D. Galloway, Catal. Today 63 (2000) 21.
[22] C.R. Vera, C.L. Pieck, K. Shimizu, J.M. Parera, Appl. Catal. A: Gen. 230 (2002) 137.
[23] J.A. Moreno, G. Poncelet, Appl. Catal. A: Gen. 210 (2001) 151.
[24] W. Stichert, F. Schüth, S. Kuba, H. Knözinger, J. Catal. 198 (2001) 277.
[25] R.A. Comelli, C.R. Vera, J.M. Parera, J. Catal. 151 (1995) 96.
[26] B.M. Reddy, P.M. Sreekanth, Y. Yamada, T. Kobayashi, J. Mol. Catal. A: Chem. 227 (2005) 81.
[27] K. Tanabe, M. Misono, Y. Ono, Stud. Surf. Sci. Catal. 51 (1989) 1909.
[28] M. Scheithauer, R.K. Grasselli, H. Knozinger, Langmuir 14 (1998) 3019.
[29] C.D. Baertsch, S.L. Soled, E. Iglesia, J. Phys. Chem. B 105 (2001) 1320.
[30] J.H. Wang, C.Y. Mou, Appl. Catal. A 286 (2005) 128.
[31] E.P. Parry, J. Catal. 2 (1963) 371.
[32] C. Morterra, G. Cerrato, M. Visca, D.M. Lenti, Chem. Mater. 3 (1991) 132.
[33] K. Ebitani, J. Konishi, H. Hattori, J. Catal. 130 (1991) 257.
[34] K. Ebitani, H. Konno, T. Tanaka, H. Hattori, J. Catal. 143 (1993) 322.
[35] T. Løften, E.A. Blekkan, Appl. Catal. A 299 (2006) 250.
[36] J.D. Henao, B.W. Sachtler, M.H. Wolfgang, J. Phys. Chem. B 109 (2005) 2055.
[37] B.Q. Xu, W.H. Sachtler, J. Catal. 167 (1997) 224.